New Methodical Approaches for the Investigation of Weathered Epoxy Resins used for Corrosion Protection of Steel Constructions

Simon Brand (Investigation) (Writing - original draft) (Visualization), Lothar Veith (Writing - review and editing) (Investigation) (Visualization), Roland Baier (Investigation) (Writing - review and editing), Christian Dietrich (Software) (Conceptualization) (Writing - review and editing), Matthias J. Schmid (Writing - review and editing), Thomas A. Ternes (Supervision) (Writing - review and editing) (Resources)

PII: S0304-3894(20)30277-6

DOI: https://doi.org/10.1016/j.jhazmat.2020.122289

Reference: HAZMAT 122289

To appear in: *Journal of Hazardous Materials*

Received Date: 2 December 2019

Revised Date: 21 January 2020

Accepted Date: 11 February 2020

Please cite this article as: Brand S, Veith L, Baier R, Dietrich C, Schmid MJ, Ternes TA, New Methodical Approaches for the Investigation of Weathered Epoxy Resins used for Corrosion Protection of Steel Constructions, *Journal of Hazardous Materials* (2020), doi: https://doi.org/10.1016/j.jhazmat.2020.122289

New Methodical Approaches for the Investigation of Weathered Epoxy Resins used for Corrosion Protection of Steel Constructions

*Simon Brand,[a] Lothar Veith,[b] Roland Baier,[c] Christian Dietrich,[a] Matthias J. Schmid,[c] *Thomas A. Ternes[a]*

Author Information

[a] Federal Institute of Hydrology, Department of Aquatic Chemistry, 56068 Koblenz, Germany
[b] Max Planck Institute for Polymer Research, 55128 Mainz, Germany
[c] Federal Waterways Engineering and Research Institute, 76187 Karlsruhe, Germany

***Corresponding Author:**
T.A. Ternes, Phone: +49 261 1306 5560. Fax: +49 261 1306 5363. E-mail: ternes@bafg.de

Graphical abstract

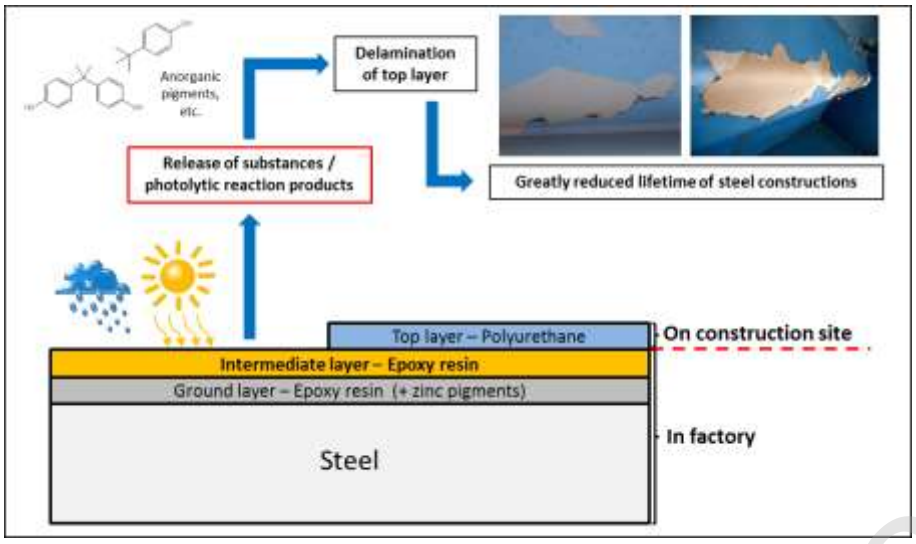

Highlights:

- Epoxy resins (EP) undergo photooxidative degradation upon UV-irradiation
- ToF-SIMS and ICP-MS prove that inorganic pigments are exposed on the surface
- LC-MS/MS analyses provide insights into degradation pathways of the EP polymer
- A mechanism for early delamination of weathered EP/PUR coating systems is proposed

Abstract

Epoxy resin coatings applied to steel constructions for corrosion protection purposes are often exposed to UV-irradiation and weathering during the construction process. Chemical alteration of the hardened coating might lead to i) the release of potentially harmful substances into the environment and ii) delamination of the polyurethane top layer. However, chemical processes and mechanisms occurring on the surfaces of exposed epoxy resin coatings are not fully understood yet. Herein, we present an innovative approach combining time-of-flight secondary ion mass spectrometry (ToF-SIMS) with inductively coupled plasma mass spectrometry (ICP-MS) and liquid chromatography mass spectrometry (LC-MS) enabling the elucidation of underlying chemical processes and the identification of released organic and inorganic photolytic products. IR-spectroscopy and experiments targeting the acidity/pH-value changes on top of weathered surfaces complement our investigations. It was confirmed that UV-A irradiation leads to photooxidative degradation of the epoxy resin and that inorganic photolytic products are exposed on the weathered surfaces. Polar moieties (hydroxyls, carbonyls, carboxyls, amines) and released metalloids form a hydrophilic surface layer, which hinders adhesion and eventually prevents profound chemical linkage of the polyurethane top layer. Thus, an early delamination of the top layer might occur very likely.

Keywords

Coating, ToF-SIMS, ICP-MS, delamination, polyurethanes

1. Introduction

Epoxy (EP) resins are commonly used as corrosion protection of steel constructions since they are relatively cheap and provide a sufficient protection against corrosion under various conditions [1, 2]. Usually, steel parts of e.g. bridges are coated with a combination of epoxy resin ground and intermediate layers at the factory, while the polyurethane (PUR) top layer is applied on the construction site when all parts are mounted and fitted in their final place [3, 4]. This procedure

ensures a coherent look of the finished structure and allows repair of smaller construction-accompanying damages of the coating. However, as a consequence, unfinished building parts are frequently exposed to weather and UV-radiation at the construction site for up to several months, leading to chemical alteration of the EP resin layer(s) [5]. As a consequence, potentially harmful substances might be released into the environment and/or delamination of the PUR top layers is promoted, which eventually reduces the lifetime of the steel construction or forces expensive repairs [6-9].

In general, 2-component EP (2C-EP) coatings are used for corrosion protection of steel constructions. Component A contains prepolymers with terminal epoxy groups (very commonly based on bisphenol A diglycidyl ether), whereas component B (the hardener) contains a variety of diamines (Figure 1). According to guideline DIN EN ISO 12944-5 [3], coating systems applied to steel constructions under appropriate conditions shall ensure corrosion protection for at least 15 years before restoration, but malfunctions with delamination of the PUR top layer after 1-3 years have been repeatedly observed by the responsible authorities. Although it is well known that epoxy resins and other polymers are sensitive to UV-radiation [10], underlying processes and mechanisms have not been fully understood yet. Most of the studies concerning EP resins either use IR-spectroscopy [11-14], which only provides information about the bulk material, or these studies are focused on topographic and performance changes such as film thickness, permeability and adhesion [15-17]. Since the coatings are polymeric materials, aside from (pyrolysis) GC-MS for detection of volatile products [18, 19] to the best of our knowledge mass spectrometric analyses have not been used to investigate the alteration of these materials so far. The aim of our study was to present new methodical approaches targeting the elucidation of the light-induced degradation mechanism of EP resins. Therefore, mass spectrometric methods (partly directly on the UV-A exposed surface, e.g. with time-of-flight secondary ion mass spectrometry (ToF-SIMS)) were used to identify degradation products, which are potentially released into the environment and/or are probably responsible for the early delamination of PUR top coatings.

2. Materials and Methods

Investigated Coatings. Four standard anti-corrosion 2C-EP resin coatings which are commonly used in Germany for both hydraulic and structural steel constructions have been investigated. Therefore, 15x15 cm² steel plates were coated according to the manufacturer's instructions by the Institute for Corrosion Protection in Dresden. To simplify (non-target) analyses and to reduce matrix effects, only EP-intermediate layers were applied to the steel plates. Samples of the educts (prepolymers and hardeners) were also available for all coatings. For more detailed information concerning the investigated coatings, see Table S1 in the supporting Information (SI).

Synthesis of a model substance. A list of used chemicals and solvents is given in Table S2 of the SI. Chemicals for the synthesis of a new model substance (see also Figure 4, preparation according to [20]) were all purchased from Sigma Aldrich and used as is. Crude product was purified with preparative liquid chromatography on silica gel (90:10% [v/v] CH_2Cl_2/MeOH) and characterized with NMR-spectrometry (see Figures S11-S12).

Artificial weathering. Samples were exposed to UV-A radiation in an indoor UV-chamber (UVA CUBE 400, for spectral range of the UV-A lamp see Figure S3) from Dr. Hönle AG (Grätelfing, Germany) and UV doses and UV intensities were recorded using the corresponding UV-Meter equipped with an optical fiber sensor (340-405 nm). Using 215 MJ/m² as reference annual UV-radiation dose in central Europe (295-400 nm),[21] UV-exposure times in the UV-A chamber could be correlated to real time exposure times.

EP resin coating samples (used for ToF-SIMS and ICP-MS, see below) were exposed to UV-A irradiation for 65 h. Irradiation of a sample for 65 h with an average power of 230 W/m² yields an energy amount of 53.82 MJ/m², which is equivalent to approximately 91 days or 3 months of real time exposure in central Europe (230 W/m² x 65 h x 3600 s/h = $53.82*10^6$ J/m²). Samples of all four EP coatings **A-D** were always irradiated simultaneously in one experiment run, so weathering conditions were always identical for all coatings.

For UV-A exposition of our model substance (used for process elucidation via LC-MS/MS, see below), a thin film (ca. 100 mg to 4 cm² surface) was applied to an object slide and exposed to UV-A light in the UV-chamber for 24 h (see also Figure S13). In parallel, a 1 µg/ml solution (MeCN) of the model substance was irradiated in a quartz glass-UV-cuvette for 24h. Irradiation of a sample for 24 h with an average power of 230 W/m² yields an energy amount of 19.87 MJ/m², which is equivalent to approximately 33 days or 1 month of real time exposure in central Europe (230 W/m² x 24 h x 3600 s/h = $19.87*10^6$ J/m²). After irradiation, the film was scraped off the object slide and dissolved in MeCN to yield a 1 µg/ml solution and both solutions were measured via LC-ESI-QToF-MS. A non-irradiated solution of the model substance served as blank and was subtracted from QToF-MS results to identify peaks correlating with UV-irradiation.

ToF-SIMS. Samples for time-of-flight secondary ion mass spectrometry (ToF-SIMS) consisted of 10 x 10 x 1 mm stainless steel plates coated with EP resins according to the manufacturer's instructions. One half of each plate was tightly covered with aluminum foil during UV-exposition, which resulted in a sharp border between exposed and original surface area on each sample. ToF-SIMS was then conducted with an IONTOF TOF.SIMS^5-NCS instrument (IONTOF GmbH, Münster, Germany) in the positive and negative secondary ion polarity of both the original and exposed surface area of each sample under conditions well below the static limit of 10^{13} ions/cm² (parameters: 30 keV Bi_3 primary ions at pulsed current of 0.11 pA; cycle time 150 µs; mass range 1-2070 u; field of view 100 x 100 µm²; primary ion dose density: 6.4 x 10^{11} ions/cm²). Stage raster analyses across the border between UV-A exposed and original surface in positive secondary ion polarity were conducted under the same analytical conditions at a 500 x 500 µm² field of view analyzing an area of 1 x 2 mm². Samples with completely untreated surfaces were also analyzed and compared to Al-covered surface areas of UV-A exposed samples to exclude contamination by the aluminum foil cover.

ICP-MS. For the analysis via inductively coupled plasma mass spectrometry (ICP-MS), 15 x 15 cm² UV-A exposed EP surfaces were wetted with ultrapure water and wiped with a rubber lip. The obtained

aqueous suspension was dried in an oven and the resulting residue was weighted and resuspended in 0.5 mL subboiled nitric acid (Suprapur, Merck). The vials were washed with approximately 10 mL deionized water (Sartorius AG, Germany), dried in an oven and then weighted again to ensure a 100 % transfer into a 10 mL tube. A microwave-assisted digestion in 1 mL subboiled nitric acid was performed (turboWave, MLS GmbH, Germany; parameters: 2.5 min 80 °C/500 W; 8 min 160 °C/850 W; 4 min 220 °C/1200 W; 9 min 220 °C/1200 W). The digested suspension was diluted to 50 mL with deionized water and the remaining particles were removed by using a 0.45 µm RC filter (Whatman Spartan, GE Healthcare Life Science, USA).

ICP-MS analysis was conducted with an Agilent 8800 triple quadrupole ICP-mass spectrometer (Agilent Technologies, Inc., Japan). The plasma and lens ICP-parameters are tuned and optimized daily (cell parameters: Mode No Gas: OctP Bias -8 V, OctP RF 140 V, Energy Discrimination 5 V; Mode He: He Flow Rate 4.3 mL/min, OctP Bias -18 V, OctP RF 180 V, Energy Discrimination 3 V; Mode H_2: H_2 Flow Rate 7 mL/min, OctP Bias -18 V, OctP RF 200 V, Energy Discrimination 0 V; Mode O_2: O_2 Flow Rate 35 %, OctP Bias -18 V, OctP RF 200 V, Energy Discrimination -4 V).

LC-MS/MS. LC-MS/MS analysis was conducted with a reverse phase C18 column and a SCIEX 5600 Triple-ToF hybrid quadrupole time-of-flight mass spectrometer (Sciex, Darmstadt, Germany), following the method described in a former publication [22]. Injection volume was always 10 µL. Evaluation of the MS-data was done in R (3.5.0) [23] and comprised peak-picking (mass range: 100-1000 Da, m/z bin: 0.02 Da, RT-range: 2-22 min, minimal intensity: 10, signal/noise ≥ 10, peak width: 5-60 sec), peak-alignment (m/z tolerance: 10 ppm, RT-tolerance: 30 sec), componentization (m/z margin: 20 ppm, RT-margin: 10 sec) and blank correction.

NMR. ^{1}H- and ^{13}C-nuclear magnetic resonance spectra (NMR) of a self-synthesized model substance were recorded with a Bruker Ascend 700 MHz NMR spectrometer (Bruker Corporation, Billerica, Massachusetts) at room temperature. Data was evaluated with TopSpin 4.0 software (Bruker Corporation). Solvent was CD_2Cl_2.

IR. Supplementary infrared spectroscopic analysis (IR) was done with a Frontier FT-IR/NIR spectrometer (Perkin Elmer, Waltham, Massachusetts), equipped with a universal ATR accessory. The 15 x 15 cm^2 coated steel plates were used as is (or after the indicated time of UV-A exposition respectively) and were directly pressed on the ATR accessory of the spectrometer. Spectra were recorded between 650 and 4000 cm^1 with 4 scans per measurement and evaluated with the corresponding software Spectrum (10.3.4, Perkin Elmer).

3. Results and Discussion

3.1. ToF-SIMS

During UV-A-exposition of the customary EP-resin coatings, the generation of a very thin, dull and dusty layer on top of the surface was observed. We suppose that by exposition to UV-A radiation chemical bonds in the polymeric EP resin matrix are being broken, leading to a degradation of the EP resin. We used the surface-sensitive time-of-flight secondary ion mass spectrometry (ToF-SIMS) technique to investigate this layer directly without any contamination through further workup. Stage raster analyses of an area containing both UV-A exposed and original surface area (see Figure 2) showed that certain ion signal intensities matched very well with the visible border between the two areas on the sample. Some fragments particularly in the very low mass range ($m/z \leq 100$) could be identified which were predominantly present at either the exposed or the original side of the sample (see Figure 3). For instance, NH_4^+ and $C_2H_8N^+$ were found at much higher intensities on the UV-A exposed sides of EP resins **A-D**, indicating that structures containing terminal amine functionalities are exposed on weathered surfaces. Opposing to this, the more unsaturated $C_2H_6N^+$ was found to be more intense on the covered surface areas of EP **A-C**, indicating that imine or non-terminal amine moieties are primarily present in the original EP. Assuming that in a non-weathered EP coating all hardener molecules have reacted, no terminal amine functionalities should be present. An increase in intensity of the NH_4^+ and $C_2H_8N^+$ signals after UV-A exposition however indicates that N-C bonds in

the EP resin are being broken and therefore more terminal amine functionalities are present on UV-A exposed surfaces.

Other examples of signals with remarkable difference in intensity in stage raster measurements can also be explained by photolytic degradation of the EP resins (see Figure 3). Aromatic fragments such as the benzyl cation ($C_7H_7^+$) were primarily found at the original surface area, which makes sense in the regard that aromatic structures have a strong absorption in the UV-A range (315-380 nm) and are therefore susceptible to photolytic degradation. Additionally, small fragments containing one oxygen atom, such as $C_2H_3O^+$ displayed a more intense signal on the UV-A exposed surface area, probably resulting from bond breaks at the isopropyl unit (opened epoxy ring). Finally, silicon organyls which were detected in EP resin **D** with high intensities on the original side of the sample were barely detected on the UV-A exposed surface area. However, signal intensity for Si^+ was elevated on the exposed side of the sample, supporting the theory that the (silicon) organic portion of the resin was degraded.

Furthermore, a comparison of the mass spectra of the UV-A exposed and the original EP resins illustrates the degradation of the organic EP resin matrix (see Figures S4-S7). For all EP resins in both positive and negative secondary ion polarity, distinct signals - mostly at higher m/z - disappeared or decreased in intensity, while new peaks at lower m/z arose. Some of the signals could be assigned to fragments of the polymeric matrix, such as Bisphenol A diglycidyl ether ($C_{12}H_{23}O_4^-$) bisphenol A ($C_{15}H_{15}O_2^-$), 4-tert-butylphenol ($C_{10}H_{13}O^-$), 4-iso-propylphenol ($C_9H_{11}O^+/C_9H_9O^-$) and other fragments of bisphenol A ($C_{14}H_{11}O_2^-$, $C_{13}H_9O_2^-$), which all of them displayed higher intensities on the original surface of the EP resin (see Table S8). Other fragments of the type $C_xH_y^+$ are also known to be fragments of Bisphenol A and were predominantly present on the original surface. Small fragments containing heteroatoms however, such as $C_3H_7O^+$, $C_2H_3O^+$, $C_2H_8N^+$, CH_4N^+, CHO^+ and NH_4^+ were found in higher intensities on the UV-A exposed EP resin surface and are probably (fragments of) degradation products [24, 25]. Furthermore, this indicates that degradation products have terminal functional groups such as amino, hydroxyl or carbonyl groups, which are easily split off during primary ion bombardment of ToF-SIMS analysis.

However, inorganic components may also be exposed on weathered surfaces due to degradation of the organic matrix of the EP resin. EP-coatings do not only consist of organic components, but also contain inorganic pigments for either coloring or functional purposes. According to the technical guideline for corrosion protection of steel constructions (TL-KOR Stahlbauten, annex C) [26], only certain types of pigments are allowed: micaceous iron oxide, titanium dioxide, zinc oxide, zinc phosphate or zinc dust as “functional pigments” and chromium oxide green, iron oxides (yellow, red, black), titanium dioxide or aluminum compounds (or carbon black or other organic pigments) as “coloring pigments”. Hence, elements present in these pigments are of primary interest.

Another advantage of ToF-SIMS analysis besides the extreme surface sensitivity is that in addition to organic molecules also inorganic elements can be detected in the same measurement. Table 1 shows detected signal intensities (positive secondary ion polarity) of various elements on top of UV-A exposed and original samples, normalized to the total ion intensity of the corresponding sample. With a few exceptions, signal intensities of elements on top of exposed surfaces were either equal to or higher than intensities on top of original surfaces. This is consistent with the idea of degradation of organic binding material and the release of inorganic pigments during UV-irradiation. For coating **D** in particular, this trend was observed, whereas for coating **A** a contrary behavior could be noticed. Since coating **A** is also the only coating showing a color change, we assume that it contains trimethoxysilyl compounds, which are added to certain coatings for the reduction of chalking, but in some cases may also increase the tendency of yellowing of the coating [27, 28].

However, the strong influence of the surrounding material on the secondary ion yield (i.e. matrix effect) in ToF-SIMS allows only a rough comparison of relative elemental contents for very similar matrices. Thus, for quantitative comparisons between different samples a method which is less affected by such matrix effects (e.g. ICP-MS with a suitable calibration, see below) is needed.

3.2. ICP-MS

Since ToF-SIMS only allows for a rough estimation of elemental contents, residues on top of UV-A exposed coatings were also checked for inorganic components with ICP-MS. Indeed, ICP-MS

measurements of HNO_3-digested residues contained high quantities of Fe, Zn, Ti, and Al (see Table 2). The fact that the residues generated on top of the coatings during UV-irradiation had the same color as the original coatings is also an indication for a (partly) inorganic character of the residues. Organic dyes with aromatic structures would be very susceptible for photolytic cleavage and should either lose or change color during UV-irradiation, which was not the case in our experiments (only coating **A** changed to a darker yellowish shade after longer exposure times). Instead, surfaces became dull and dusty, which resembles the process of chalking of varnishes and paintings [29].

Considering the color of the applied EP-coating (**A**: yellowish white, **B**: black, **C**: red, **D**: grey metallic; see also Figure S9), elevated concentrations of these metals are plausible. Coating **D** for example, which showed by far the highest concentration of Al is also the only coating with a metallic appearance, which is the main purpose Al pigments are used for. It is also the only coating where micaceous iron oxide as ingredient is explicitly declared, which explains the high Fe concentrations. The yellowish and red color of coatings **A** and **C** may be generated by the corresponding iron oxide pigment (moderate to high Fe concentration), while the black color of coating **B** is probably caused by carbon black or another organic pigment (very low Fe concentration). Ti had the highest concentration in coating **A,** which also has the lightest color of all coatings (TiO_2 is a very common white pigment). Elevated Zn concentrations were present in all coatings, probably due to its prominent usage as “functional pigment”, while Cr concentrations were negligibly small. Since chromium pigments are only allowed/used for greenish colored EP coatings, this was an expected result.

However, also some other unexpected metals such as Ni, Cu or Mn were detected with ICP-MS in certain samples (see Table S10). Increased Ni concentration in coating **A** may be explained by the usage of a yellow pigment called “nickel titanate”, a nickel titanium oxide; this would also correlate with increased Ti concentrations found in coating **A**. However, we are not sure about the surprisingly high concentrations of Mn in coatings **C** and **D** and increased Cu concentrations among all four coatings. Concentrations of other elements such as Sn, V, Co, Se, Mo, Ag, Cd and Sb were below or near the limit of detection (LOD, see Table S10).

The detection of metalloids such as Ni, Cu, Mn and also Zn on top of UV-A exposed EP surfaces is concerning since they can be washed off and could contaminate the (aquatic) environment. Unlike larger oligomeric fragments, the small and polar or ionic pigments and salts are more easily leached into the environment, especially when they are exposed on the surface. Certain species and salts of these metals are known to be highly toxic to water organisms. Furthermore, the release of small organic contaminants such as 4-tert-butylphenol [A.M. Bell, S. Buchinger, Federal Institute of Hydrology, Koblenz, Germany; pers. comm.] or bisphenol A derivates [9] can pose environmental hazards. The question arises, why the identified metalloids and organic contaminants are used in EP coatings although they are released into the into the (aquatic) environment, and why they are not listed in the corresponding technical guideline [26].

3.3. Model substance for process elucidation

To simplify investigations and to get a general idea of *how* the degradation of the EP resin takes place during UV-irradiation, a non-polymeric model substance with the smallest possible cross-linking level was synthesized according to the procedure described by Cepanec et.al.[20] (Figure 4). Coupling of bisphenol A diglycidyl ether with a secondary mono-amine (*N*-benzylmethylamine) led to product **1** as a model for a "hardened epoxy resin", but with the advantage that this model compound is soluble in organic solvents (MeCN) and therefore amenable to LC-MS/MS approaches. The molecular structure was confirmed by NMR (see Figure S11 and S12).

Assuming that the underlying mechanism is a photooxidative degradation, as proposed by Lin et al.[11], four major sites of the model substance are predicted where the initiation step (hydrogen abstraction) could occur (**I-IV**, see also Figure 4 and Figure S14). While site **I** would primarily yield aldehydes and alcohols, site **II** would yield carboxylic acids, methyl ethers and methylamines, site **III** aldehydes, amines and amides and site **IV** amines, amides and benzaldehyde (see Figures S15-18).

The five most intense signals in ESI-(+)-mode after UV-A exposition of the model substance **1** are shown in Table 3, along with suggestion of the chemical formula and chemical structure (Figure 5). It was found that the aryl-O-C-bond and the N-C-bonds in particular were susceptible to UV-A

irradiation, as features **2** and **3** were corresponding to proposed photooxidative degradation products **IVa** and **Ia** respectively (amine and phenol). Features **2** and **4** belong to the same photolytic product, but were detected as two different features since double-charged ions were generated in the ion source. Double-charged ions could be observed multiple times for substances with two (or more) amino-groups, as those are readily protonated in the ESI source.

Interestingly, there were also few photolytic products with a higher molecular mass than the initial starting product (e.g. benzylation of the model compound at one amino group (**6**)) and which were not directly predicted by the mechanism of Lin et al. This indicates, that **1** is not only degraded into smaller molecules, but that degradation products generated during UV-irradiation can combine with the surrounding matrix or other photolytic products to form new higher molecular weight compounds (especially during the termination step of the photooxidative degradation, which is basically a recombination of two radicals). Furthermore, homolytic bond cleavage through high energy UV-radiation cannot be ruled out. Compound (**5**) was identified as a photolytic product, where we suggest an *intra*molecular reaction through a six-membered transition state (see Figure S19). Although it is questionable if this reaction would also take place in a "real" polymeric epoxy resin (the benzyl radical involved in it is a product of this very specific amine used for the synthesis of **1**), investigations with the model substance emphasize three main results: photooxidative degradation can be confirmed as possible degradation mechanism, N-C-bonds and aryl-O-C bonds are most likely cleaved (yielding amines and phenolic structures) and photolytic products contain more terminal functional groups such as alcohols, amines etc. which is confirmed by ToF-SIMS.

3.4. IR-spectroscopy and acidity

Infrared spectra (IR) of the surface of UV-A exposed coatings (see Figures S20-S23) matched well with observations made in previous publications (generation of two new peaks at around 1730 cm^{-1} and 1640 cm^{-1}, assigned to C=O oscillation in ketones/aldehydes/carboxylic acids/esters and amides respectively) [12, 13, 16]. In order to characterize the changes to the polymeric material under other conditions than UV-A irradiation, one EP resin (**A**) was also studied with ATR-FTIR spectroscopy after

exposition to UV-B and UV-C radiation, Xenon weathering (DIN EN ISO 11507), atmospheric weathering and thermolytic degradation at 130°C (see Table S24).

For all these weathering conditions, the same new peaks associated with carbonyl groups were found - albeit with different relative intensities. Usually, the peak at about 1730 cm^{-1} was more intense than the peak at about 1640 cm^{-1}, except for the UV irradiated sample, where the relative intensity of the two peaks changed. The degradation products formed might be aldehydes, ketones or carboxylic acid derivatives such as esters, amides or ammonium carboxylates. Although some of these weathering conditions were relatively harsh and do not naturally occur (UV-C irradiation is filtered in the atmosphere and does not reach the earth and surface temperatures of a black coating on a hot summer day will not exceed 80 °C), these experiments show that altering of EP resins by other spectral regions of the sunlight and increased temperature may not be ruled out. However, the increase of C=O signal intensity in IR was fastest and most significant under UV exposure and corresponding proposed photolytic degradation reactions have been summarized by Lin et al. [11] (see also Figures S14-S18).

Furthermore, EP resin **A** was also studied after leaching in aerated distilled water at 60 °C without prior UV-irradiation. After certain intervals, the pH value of the water was measured, as shown in Table 4. The pH value decreased over time, which corresponds to results from Krauklis et al. [30], although we do not think that leaching of HCl is responsible for the pH decrease. Instead, it has been observed that small volatile degradation products such as acetaldehyde and benzaldehyde are generated during thermal degradation [R. Baier, Federal Waterways Engineering and Research Institute, Karlsruhe, Germany; pers. comm.], which can be oxidized to their corresponding carboxylic acids in presence of oxygen. During long-time exposure experiments, these small acids accumulate in water over the course of time and might be therefore responsible for the pH decrease. However, if UV-radiation and/or high temperature is involved, the straight generation of carboxyl moieties is also possible (see Figure S16), despite not being responsible for a decrease of the pH-value. Carboxyl moieties on top of a weathered coating would be bound covalently to the polymer surface and thus be immobile. Upon dissociation (COO^- and H^+), hydronium ions could not leave the surface/eluate

interface without generating an electrostatic potential (negative polarization of the coating surface, positive polarization of the eluate), which is rather unlikely.

Eluates of our model substance **1** before and after 24h of UV-exposition exhibited no pH difference, which is consistent with both of our assumptions: i) short time elution without proper conditions (elevated temperatures, high oxygen saturation of the water) does not lead to a pH decrease and ii) carboxylic moieties formed on top of weathered surfaces would not significantly increase the pH value due to electrostatic interactions.

Further evidence for the presence of acidic groups on top of weathered EP resins was investigated using the catalytic discoloration of methylene blue [31] (see Table S25 and Figures S26-S27). In the described method methylene blue is discolored in a reduction with titanium(III)chloride. While this reaction takes about 10 s in absence of a catalyst, discoloring is instantaneous when catalyzed by oxalic acid or ammoniumoxalate. We tested eluates (distilled water) sampled from the surface of EP resin **A** after 1 year of atmospheric weathering (sunlight, rain) and observed the same catalytic acceleration of the reaction as described in [31].

We also found that the same catalytic effect could be observed when using a variety of other substituted amino acids (glycine and EDTA) and substituted benzoic acids (sodium salicylate, ammonium isophtalate and ammonium 4-hydroxybenzoate). Although this does not necessarily mean that one of these substances is actually present on top of the weathered EP resin surface, this is seen as an indicator that acidic moieties were generated during weathering of the EP resin.

3.5. Delamination

To understand why in some cases PUR top coatings applied to weathered EP intermediate layers delaminate after a short period of time, it is essential to understand how the PUR adheres to an intact EP in the first place (Figure 6 (a)). When using a 2-component polyurethane coating (2C-PUR), the two primary ingredients are diisocyanates and a polyacrylates with free hydroxyl groups. These hydroxyl groups react with the isocyanate groups and form a polymeric, three dimensional urethane network. However, either a) secondary amine groups of the EP polymer, b) free hydroxyl groups of

the EP polymer or c) primary amine groups of unreacted EP hardener may also react with free isocyanate groups of the PUR, forming a chemical bonding between PUR and EP layers which improves the stability of the coating system.

In case of a weathered EP intermediate layer, our results confirmed that the organic matrix of the EP is cleaved during UV exposition and that inorganic pigments are exposed on the surface. These residues, together with morphologic changes on top of the surface (e.g. increase of roughness and heterogeneity due to erosion, micro-cracks and thickness loss)[16] might be a simple physical reason for the delamination, since adhesion on top of a weathered and dusty surface is inferior to adhesion on top of a smooth and clean surface of a non-weathered EP coating. However, more importantly, inorganic residues (minerals/salts) and the photolytically altered EP (hydroxyl, carboxyl, and amine/amide groups) form a hydrophilic surface layer, which may take up water molecules from humidity or rain events. Upon application of the PUR top layer, the water molecules react with the free isocyanate groups of the PUR top coating and form an unstable carbamic acid, which dissociates into CO_2 and an amine. As consequence, these amines may react with other isocyanate groups of the PUR, resulting in an intrinsic reaction within the PUR layer instead of bonding to the EP intermediate layer (Figure 6 (b)). Furthermore, the redundant CO_2 causes blistering within the PUR layer, which also reduces the cross-linking and creates pores through which further water and UV radiation can reach the EP layer. Malfunctioning EP-PUR coating systems very often show this kind of blistering prior to extensive delamination of the PUR top coating (see Figure S28), which supports our theory.

Considering this model, it does not surprise that manufacturers recommend washing surfaces of steel constructions with an alkaline wash primer prior to application of a new layer of coating, presumably to remove (acidic) photolytic residues. Recommended procedure consists of pressure washing the EP intermediate coating with water, followed by application of the wash primer with decent dwell time before pressure washing it again. The PUR top coating is then applied to the dry EP intermediate coating. However, experiences have shown that washing does not guarantee a good adhesion of the top layer, while light abrasive cleaning (“sweeping”) leads to promising results. This again is consistent with our delamination theory, since some of the degraded organic material and

hydrophilic salts may be removed with water, while some of the insoluble salts and (firmly attached) oligomeric groups cannot be removed with water or even alkaline solutions. Although sweeping of the weathered EP intermediate is a successful countermeasure to this problem, abrasive cleaning a) reduces the overall film thickness of the protective coating, potentially making it less effective and b) demands an additional and expensive work step, since the removed material must not get into the environment.

4. Conclusion

New approaches targeting analysis directly on top of UV-A exposed anti corrosion EP resin surfaces (ToF-SIMS, ICP-MS), together with supplementary IR spectroscopy and investigations of a self-synthesized model EP resin allowed us to identify components of the photolytic residues and to draw conclusions about the underlying processes (different photooxidative degradation pathways). The results explain why for EP coatings adhesion of PUR top coatings on top of a weathered and untreated intermediate layer is inferior to adhesion on top of a smooth and clean surface of a non-weathered EP. The main mechanism identified here is the formation of a thin hydrophilic film (carboxyl, ammonium and hydroxyl groups; inorganic salts) which is easily hydrated by moisture or rain events. The water molecules within this film lead to detrimental side reactions of the PUR top coating, reducing the cross-linking of the polymer layers and generation of CO_2 bubbles. Since some of the hydrophilic groups are attached firmly to the EP intermediate layer, washing sometimes does not restore the surface to its original state. Exposed inorganic particles and metalloids however may be washed off and could contaminate the (aquatic) environment.

Author Contribution Statement:

Simon Brand: Investigation, Writing – Original Draft, Visualization; **Lothar Veith**: Writing – Review and Editing, Investigation, Visualization; **Roland Baier:** Investigation, Writing – Review and Editing; **Christian Dietrich:** Software, Conceptualization, Writing – Review and

Editing; **Matthias J. Schmid:** Writing – Review and Editing; **Thomas A. Ternes:** Supervision; Writing – Review and Editing, Resources.

Declaration of Interest

All authors declare no competing interest.

5. Acknowledgements

The authors thank Marcus von der Au (Federal Institute of Hydrology, BfG) for acquisition of ICP-MS measurements and Manfred Wagner (Max Plank Institute for Polymer Research, MPI-P) for acquisition of NMR measurements. We also thank Birgit Kocher and Małgorzata Schröder (both Federal Highway Research Institute, BASt) for valuable discussions. Financial Support by the Federal Ministry of Transport and Digital Infrastructure (BMVI) for the Network of Experts "Knowledge – Ability – Action" is gratefully acknowledged.

6. Abbreviations

ATR-FTIR, attenuated total reflection Fourier transform infrared spectroscopy; CH_2Cl_2, dichloromethane; EDTA, ethylenediaminetetraacetic acid; EP, epoxy or epoxide; ESI, electrospray ionization; HNO_3, nitric acid; ICP-MS, inductively coupled plasma mass spectrometry; LC-MS, liquid chromatography mass spectrometry; LOD, limit of detection; MeOH, methanol; MeCN, acetonitrile; NMR, nuclear magnetic resonance spectrometry; PUR, polyurethane; QToF-MS, quadrupole time-of-flight mass spectrometry; RT, retention time; ToF-SIMS, time-of-flight secondary ion mass spectrometry; UV, ultraviolet light/radiation.

7. Associated Content

Supporting Information (SI)

8. References

[1] P.A. Schweitzer, Paint and Coatings - Applications and Corrosion Resistance, CRC Press, Boca Raton (Florida), 2005.
[2] P.A. Sørensen, S. Kiil, K. Dam-Johansen, C.E. Weinell, Anticorrosive coatings: a review, Journal of Coatings Technology and Research, 6 (2009) 135-176.
[3] DIN EN ISO 12944-5: Paints and varnishes - Corrosion protection of steel structures by protective paint systems - Part 5: Protective paint systems, (2018).
[4] F. Bayer, A.W.H. Capell, G. Gormanns, O. Nicolai, J. Pflugfelder, Broschüre: Korrosionsschutz von Stahlbauten durch Beschichtungssysteme, (2010).
[5] D. Gurack, G. Krüger, A. Krotzek, A. Rudolf, Adhäsionsverhalten zwischen bewitterten 2K-EP-Beschichtungen und 2K-PUR-Beschichtungen – Einfluss der Bewitterung, 80 (2011) 627-635.
[6] A. Gelhaar, A. Schneider, Zur Problematik der Zwischenbewitterung von Epoxidharz-Teilbeschichtungen an Brückenbauwerken, Stahlbau, 76 (2007) 131-142.
[7] W.P. Öchsner, R. Schmidt, Auf der Suche nach optimaler Zwischenhaftung, Farbe & Lack, 5 (2007) 146.
[8] G. Motzke, R. Konermann, Haftung von PUR-Deckbeschichtungen auf bewitterten EP-Beschichtungen – Haftungsfragen für Unternehmer und Hersteller, Stahlbau, 76 (2007) 771-777.
[9] E.L.M. Vermeirssen, C. Dietschweiler, I. Werner, M. Burkhardt, Corrosion protection products as a source of bisphenol A and toxicity to the aquatic environment, Water Research, 123 (2017) 586-593.
[10] J.F. Rabek, Polymer Photodegradation - Mechanisms and experimental methods, Champman & Hall, London (UK), 1995.
[11] S.C. Lin, B.J. Bulkin, E.M. Pearce, Epoxy resins. III. Application of fourier transform IR to degradation studies of epoxy systems, Journal of Polymer Science: Polymer Chemistry Edition, 17 (1979) 3121-3148.
[12] V. Bellenger, J. Verdu, Photooxidation of amine crosslinked epoxies I. The DGEBA–DDM system, Journal of Applied Polymer Science, 28 (1983) 2599-2609.
[13] V. Bellenger, J. Verdu, Oxidative skeleton breaking in epoxy–amine networks, Journal of Applied Polymer Science, 30 (1985) 363-374.
[14] G.A. Luoma, R.D. Rowland, Environmental degradation of an epoxy resin matrix, Journal of Applied Polymer Science, 32 (1986) 5777-5790.
[15] W.R.R. Park, J. Blount, Oxidative Degradation of Epoxy Resin Coatings, Industrial & Engineering Chemistry, 49 (1957) 1897-1902.
[16] A. Rezig, T. Nguyen, D. Martin, L. Sung, X. Gu, J. Jasmin, J.W. Martin, Relationship between chemical degradation and thickness loss of an amine-cured epoxy coating exposed to different UV environments, Journal of Coatings Technology and Research, 3 (2006) 173-184.
[17] S.B. Lyon, R. Bingham, D.J. Mills, Advances in corrosion protection by organic coatings: What we know and what we would like to know, Progress in Organic Coatings, 102 (2017) 2-7.
[18] J.M. Stuart, D.A. Smith, Some aspects of the degradation of epoxide resins, Journal of Applied Polymer Science, 9 (1965) 3195-3214.
[19] B.D. Gesner, P.G. Kelleher, Oxidation of bisphenol A polymers, Journal of Applied Polymer Science, 13 (1969) 2183-2191.
[20] I. Cepanec, M. Litvic, H. Mikuldas, A. Bartolincic, V. Vinkovic, Calcium trifluoromethanesulfonate-catalysed aminolysis of epoxides, Tetrahedron, 59 (2003) 2435-2439.
[21] Atlas Material Testing Solutions, Weathering Testing Guidebook, (2001) http://www.strenometer.dk/Files/Downloads/Guidebook.pdf.
[22] S. Brand, M.P. Schlüsener, D. Albrecht, U. Kunkel, C. Strobel, T. Grummt, T.A. Ternes, Quaternary (triphenyl-) phosphonium compounds: Environmental behavior and toxicity, Water Research, 136 (2018) 207-219.
[23] R Development Core Team, R: A language and environment for statistical computing., (2008) http://www.R-project.org.

[24] J.A. Treverton, A.J. Paul, J.C. Vickerman, Characterization of adhesive and coating constituents by time-of-flight secondary ion mass spectrometry (ToF-SIMS). Part 1: Epoxy-terminated diglycidyl polyethers of bisphenol-A and propal-2-ol, 20 (1993) 449-456.
[25] F. Awaja, P.J. Pigram, Surface molecular characterisation of different epoxy resin composites subjected to UV accelerated degradation using XPS and ToF-SIMS, Polymer Degradation and Stability, 94 (2009) 651-658.
[26] S.K. Gurung, S. Thapa, A. Kafle, D.A. Dickie, r. Giri, Suzuki Cross Coupling with Cu (4), Org. Lett., 16 (2014) 1264-1267.
[27] V. Malshe, G. Waghoo, Weathering study of epoxy paints, 2004.
[28] N. Rajagopalan, A. Khanna, Effect of Methyltrimethoxy Silane Modification on Yellowing of Epoxy Coating on UV (B) Exposure, 2014.
[29] H.G. Völz, G. Kaempf, H.G. Fitzky, A. Klaeren, The Chemical Nature of Chalking in the Presence of Titanium Dioxide Pigments, in: Photodegradation and Photostabilization of Coatings, AMERICAN CHEMICAL SOCIETY, 1981, pp. 163-182.
[30] A.E. Krauklis, A.T. Echtermeyer, Mechanism of Yellowing: Carbonyl Formation during Hygrothermal Aging in a Common Amine Epoxy, 10 (2018) 1017.
[31] N. Rukmini, B.S. Chalam, Y. Rao Pulla, Detection of oxalic acid by catalytic reaction, Fresenius Zeitschrift für analytische Chemie, 290 (1978) 320-320.

Figures and Tables

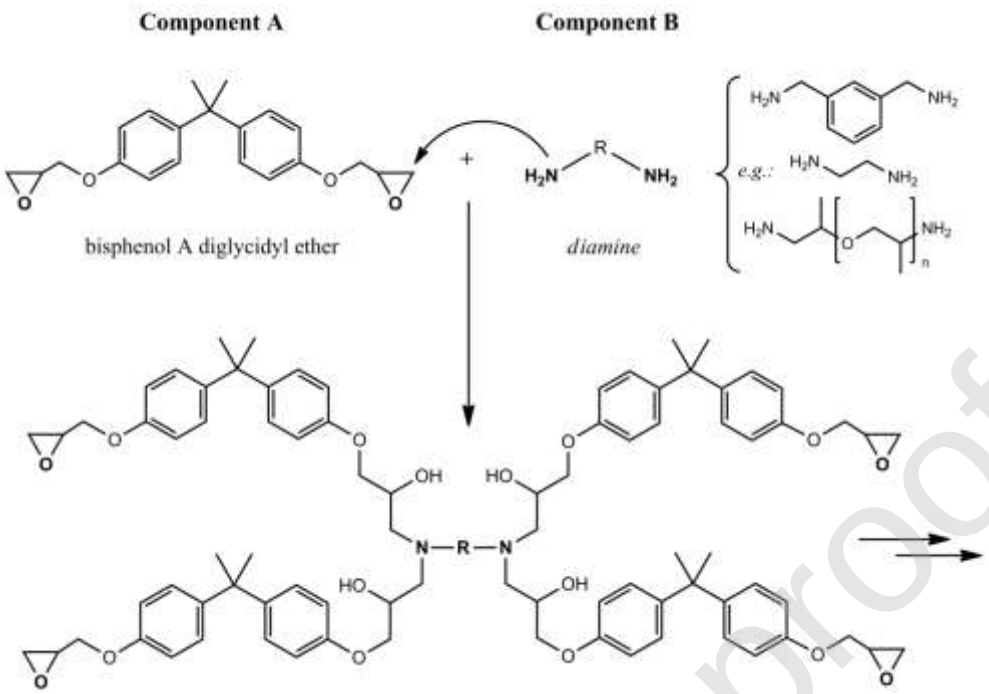

Figure 1: Illustration of the curing reaction of a 2-component epoxy resin (2C-EP), using the example of bisphenol A diglycidyl ether and a generic diamine.

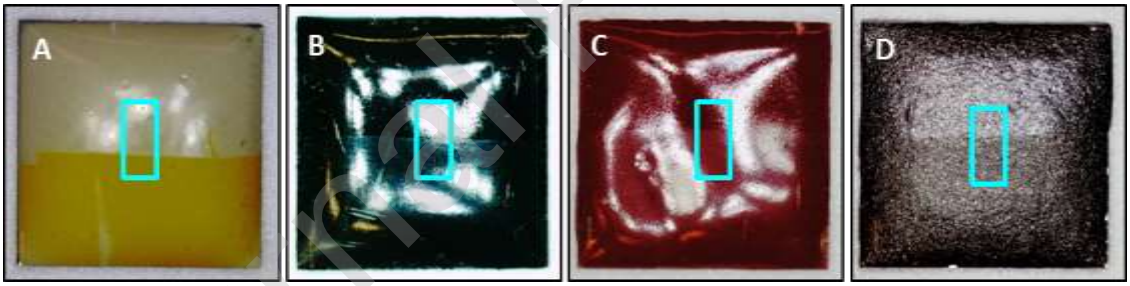

Figure 2: Original (top) and UV-A exposed (bottom) surface areas of coatings **A-D** on 1 x 1 cm² steel plates. The cyan rectangle marks the area screened by stage raster ToF-SIMS analysis.

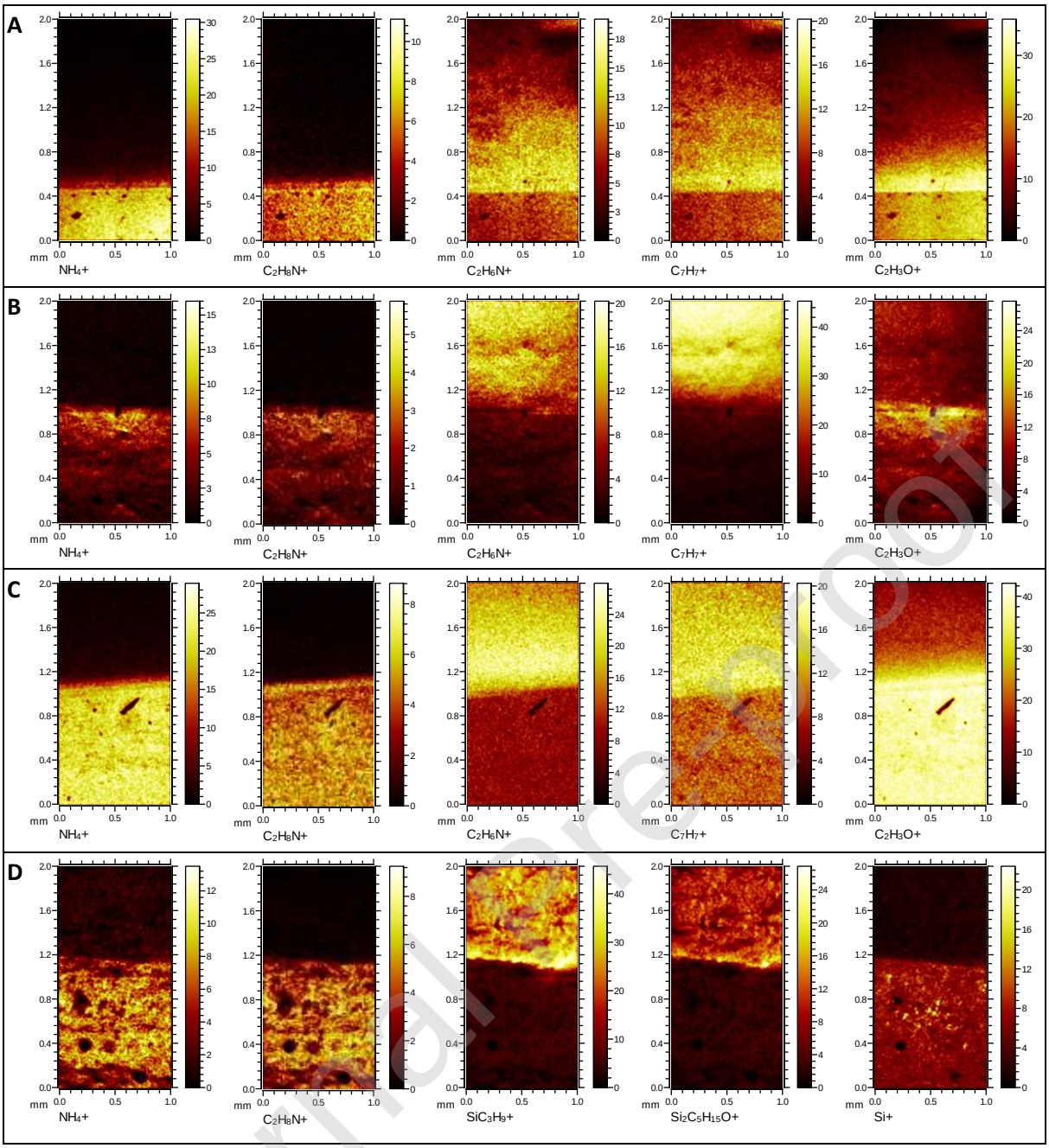

Figure 3: ToF-SIMS stage raster analyses at the border region between original and UV-A exposed surface areas of coatings **A-D** on steel plates reveal differences in relative signal intensities for selected ion distributions. In each individual image, UV-A exposed areas are depicted below and original areas above the visible border (compare also with Figure 2).

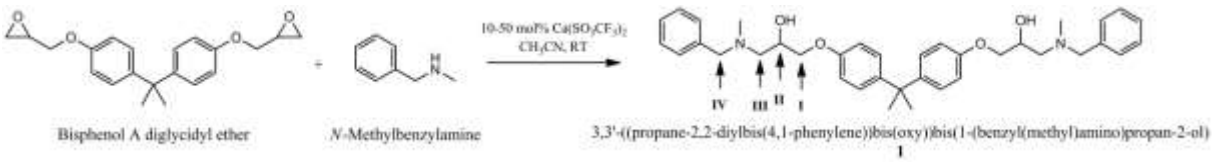

Figure 4: Synthesis of model compound **1** as a non-polymeric, soluble „epoxy-resin“ and the four possible initiation sites for photooxidative degradation (**I-IV**), as proposed by Lin et al.

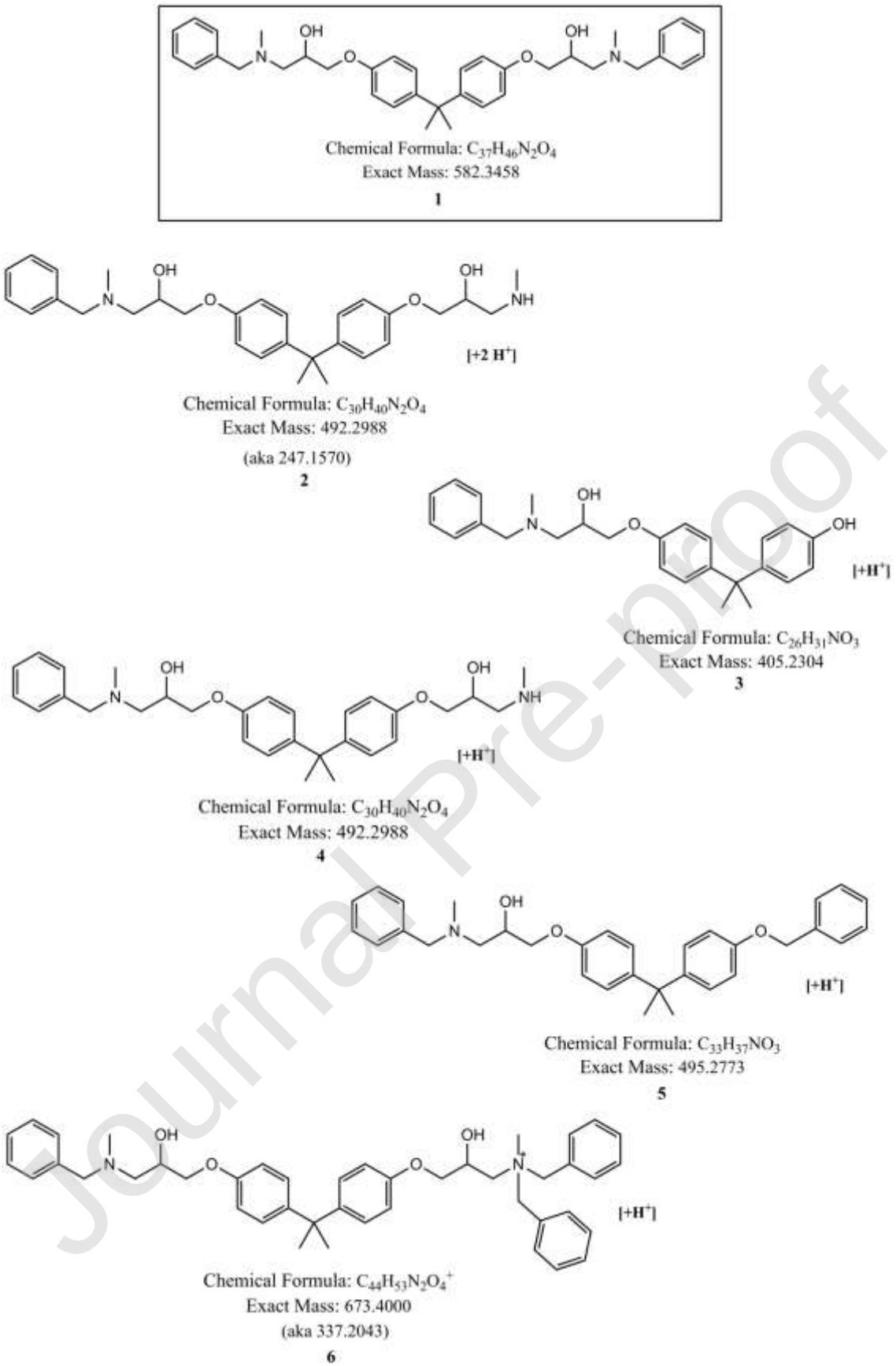

Figure 5: Proposed chemical structures of the major photolytic products (ordered by LC-MS signal intensity) of the synthesized molecule **1**.

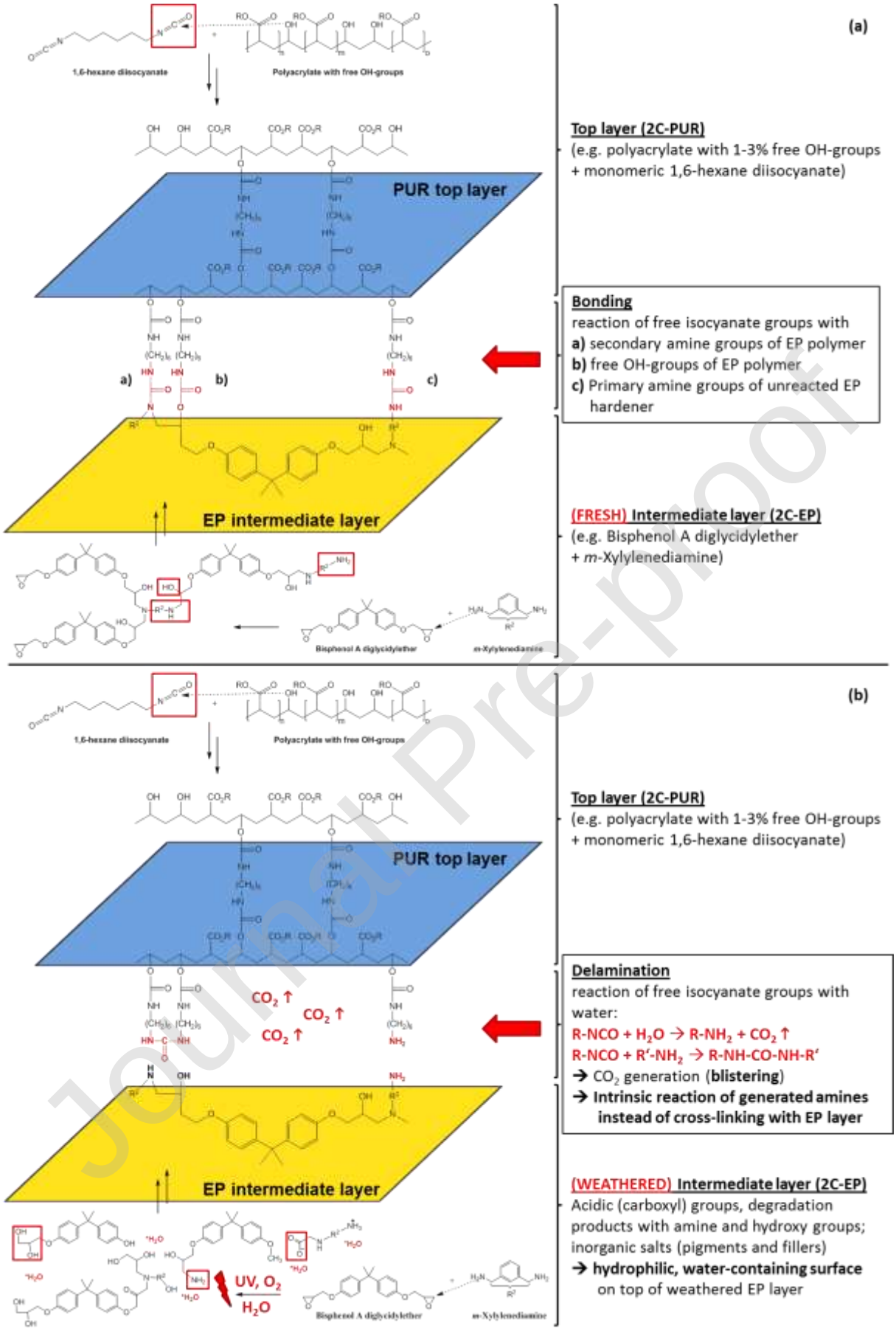

Figure 6: Schematic illustration of chemical processes during painting of PUR top layer on top of a fresh (**a**) and weathered (**b**) EP intermediate layer.

Table 1: Semi-quantitative overview of selected elements on the surfaces of coatings **A**-**D** before and after UV-A exposition. Signal areas were normalized to the total ion intensity of each sample. Comparison is only valid within a row (element).

Area Norm. TIC		**A**		**B**		**C**		**D**	
	Mass (u)	original	UV-exposed	original	UV-exposed	original	UV-exposed	original	UV-exposed
Ti+	47.9487	1.03E-05	9.82E-07	2.56E-06	2.14E-06	2.19E-06	1.50E-06	9.25E-07	2.39E-06
Mn+	54.9367	6.68E-06	9.82E-07	1.23E-05	4.15E-06	7.65E-06	1.43E-05	6.17E-06	5.15E-05
Fe+	55.9316	2.52E-05	3.93E-06	6.70E-05	3.85E-05	1.16E-05	9.89E-05	1.30E-05	8.93E-05
Cu+	62.929	4.78E-06	3.93E-06	6.39E-06	7.96E-06	3.85E-06	2.36E-05	2.78E-06	1.28E-05
Zn+	63.9263	5.18E-06	1.96E-06	6.39E-06	8.69E-06	4.62E-06	4.35E-06	3.39E-06	5.89E-06
Al+	26.9795	5.13E-05	5.89E-06	1.07E-04	3.09E-05	1.96E-06	3.82E-05	4.01E-06	2.19E-04
Cr+	51.9416	3.69E-06	1.96E-06	4.86E-06	5.42E-06	4.68E-06	5.08E-06	2.47E-06	1.02E-05
Ni+	57.938	8.97E-06	9.82E-07	1.64E-05	6.15E-06	9.19E-06	3.42E-06	6.78E-06	1.17E-05
Si+	27.9743	3.21E-04	2.97E-03	7.84E-04	1.72E-03	5.57E-06	8.80E-04	1.03E-03	8.22E-03

Table 2: Element concentrations determined with ICP-MS in the fine, powdery residue on top of epoxy resin coatings **A-D** after UV-A exposition. Each sample was measured as triplicate; the full list of determined elements can be found in Table S10.

	A (yellowish white) [mg/kg]	**B** (black) [mg/kg]	**C** (red) [mg/kg]	**D** (grey metallic) [mg/kg]
Fe	431 ± 4	74 ± 1	800 ± 200	1590 ± 9
Zn	1380 ± 20	800 ± 10	900 ± 200	2530 ± 30
Ti	92 ± 3	5.3 ± 0.3	5.5 ± 0.1	15.3 ± 0.4
Al	572 ± 4	200 ± 10	377 ± 3	6400 ± 200
Cr	4.47 ± 0.04	0.90 ± 0.03	2.50 ± 0.09	2.93 ± 0.07

Table 3: The five major photolytic products of model compound **1** with molecular formulas, ordered by their LC-MS signal intensities (**1** as comparison). The corresponding proposed chemical structures are shown in Figure 5.

(ESI+)	**Feature [m/z]**	**RT**	**Intensity**	**Formula**	**Deviation**

		[min]	[counts]		[ppm]
1	583.3530	7.36	237000	**Starting Product [M+H$^+$]** $C_{37}H_{46}N_2O_4$ [+H$^+$]	-0.5
2	247.1574	6.43	48700	$C_{30}H_{40}N_2O_4$ [+2H$^+$]	-0.6
3	406.2381	8.28	43200	$C_{26}H_{31}NO_3$ [+H$^+$]	-0.8
4	493.3059	6.43	33100	$C_{30}H_{41}N_2O_4$ [+H$^+$]	-0.3
5	496.2848	11.00	28900	$C_{33}H_{37}NO_3$ [+H$^+$]	-0.1
6	337.2036	8.30	25300	$C_{44}H_{53}N_2O_4^+$ [+H$^+$]	+1.4

Table 4: Exposure times of EP **A** to aerated distilled water at 60 °C and corresponding pH-values.

Time of water exposure at 60 °C [h]	0	100	1440	2100
pH of the water	5.6	4.6	4.4	4.1